Case Studies of African Wave Disturbances in Gridded Analyses

LEONARD M. DRUYAN

Center for Climate Systems Research, Columbia University, New York, New York

PATRICK LONERGAN

Science Systems and Applications, Inc., NASA/Goddard Institute for Space Studies, New York, New York

JUDAH COHEN

Department of Civil and Environmental Engineering, Massachusetts Institute of Technology, Cambridge, Massachusetts

(Manuscript received 18 November 1996, in final form 13 February 1997)

ABSTRACT

African wave disturbances (AWDs), an important trigger of Sahel summer rainfall, are studied using ECMWF gridded datasets for July and August 1987 and 1988. Power spectra of time series of 700-mb meridional winds near Niamey taken from analyses at both 2° × 2.5° and 4° × 5° horizontal resolution are compared to spectra based on Niamey station data. In addition, spatial distributions of meteorological fields at both resolutions are discussed for three case studies, including the synoptic features of several AWDs. Additional examples are presented from GCM simulations at comparable horizontal resolutions. While vertical motion and divergence centers were more extreme at 2° × 2.5°, many of the deduced characteristics of an AWD were similar at both resolutions. The higher-resolution analyses and simulation show a sharp transition across wave troughs between lower-tropospheric convergence (uplift) on the west and divergence (subsidence) on the east for several AWDs. For the two more southerly AWDs analyzed here, uplift associated with the convergence ahead of the trough appears to be displaced to the southwest at midtropospheric altitudes. Twice-daily July–September precipitation at Niamey is weakly, but significantly, correlated with corresponding time series of ECMWF analyzed vertical motion at nearby grid points.

1. Introduction

An early description of African wave disturbances (AWDs) with periods of generally 3–5 days was given by Burpee (1972), based on spectral analyses of tropospheric meridional winds observed at selected stations in northern Africa. This synoptic feature of the Sahel's summer climate is significant because much of the season's rainfall occurs in organized squall lines (Lamb and Peppler 1991) that are imbedded within an AWD (Fortune 1980; Landsea and Gray 1992). In fact, Duvel (1988) determined that about 50% of the interdiurnal variance of outgoing longwave radiation representing Sahel summer convection is accounted for by spectral periodicities of 2.6–8.4 days, an interval that includes the periods of observed AWDs (Reed et al. 1977). Reed et al. (1988a) reported that the ECMWF T106 resolution operational system was quite successful in tracking and forecasting the movement of AWDs during August and September 1985. The three-dimensional structure of spectral properties of circulation and temperature associated with AWDs is described by Reed et al. (1988b) based on the same ECMWF analyses, gridded at 3° × 3° horizontal resolution. They concluded that these data realistically portrayed AWD characteristics and "have much potential value for documenting wave behavior . . . and for improving the diagnosis of basic physical mechanisms."

To study the contribution of AWDs to the interannual variability of precipitation at Niamey, Druyan et al. (1996) (hereafter DLS) used ECMWF observed datasets gridded at 4° latitude by 5° longitude. Several benefits of the the 4 × 5 arrays were perceived, even though the same datasets are available at the spatial resolution of 2° latitude by 2.5° longitude. For example, the burden of data handling for twice daily global arrays makes it attractive to find applications for the 4 × 5 data, which are archived at the Data Assimilation Office of the NASA/Goddard Space Flight Center. Moreover, representation of the various meteorological distributions at the coarser spatial resolution facilitates comparisons with simulations represented on a similar grid by the

Corresponding author address: Dr. Leonard M. Druyan, Center for Climate Systems Research, Columbia University, Armstrong Hall, 2880 Broadway, New York, NY 10025.
E-mail: ldruyan@giss.nasa.gov

standard climate model of the NASA/Goddard Institute for Space Studies (GISS GCM) in the context of an ongoing project.

We have recently begun to analyze GISS GCM simulations made at $2^\circ \times 2.5^\circ$ horizontal resolution, lending greater motivation to diagnostic studies of AWDs with the corresponding $2^\circ \times 2.5^\circ$ ECMWF analyses. The purpose of this paper, therefore, is to compare and contrast the representation of rain-producing synoptic features over the Sahel, especially AWDs, at the two resolutions in analyses and GCM simulations.

We note at the outset that evaluation of the $2^\circ \times 2.5^\circ$ analyses raises several questions. For a data-sparse region such as West Africa, where the spacing between real-time observing stations can be greater than the grid spacing at either resolution, the gain achieved by a straightforward interpolation of observations to the higher-resolution grid is not obvious. However, Trenberth (1992) points out that higher spatial resolution structures are created by the ECMWF analysis scheme because it uses 6-h model predictions as ''first-guess'' fields and model integrations as part of the data interpolation. Moreover, some of these features may be influenced by the specified surface topography (T. Palmer 1996, personal communication). Finally, assimilation of satellite-derived data sometimes enhances the coverage provided by ground stations. To aid in the assessment of any advantages of the $2^\circ \times 2.5^\circ$ analyses, comparisons are here made versus impacts resulting from these resolution differences in GISS GCM simulations. Synoptic details unique to the $2^\circ \times 2.5^\circ$ simulations reflect the potential benefits of a more realistic representation of topography and sharper horizontal gradients of model variables. Parallels between resolution effects for analyses and simulations lend confidence to their meteorological significance since results from the two model versions are not just interpolation differences.

With the foregoing arguments in mind, we describe several case studies of synoptic patterns over West Africa during August 1988, including the analysis of several AWDs, and compare their depictions at two horizontal resolutions. The advantages of the $2^\circ \times 2.5^\circ$ representations, especially with reference to the basic conclusions discussed by DLS, are considered in the context of atmospheric conditions over northern Africa for three synoptic times and with reference to the properties of July and August 1987 and 1988 wind spectra and twice daily rainfall accumulations during July–September 1988.

2. Spectra of 700-mb meridional wind

AWDs are detected as spectral peaks at periods of 3–6 days in time series of the 700-mb meridional wind (v7) over West Africa (Burpee 1972; DLS). In DLS we compared power spectra of Niamey radiosonde v7 during July and August versus collocated time series from $4^\circ \times 5^\circ$ ECMWF analyses (Fig. 1). Fewer spectral maxima and, in particular, the absence of high amplitudes that are present in the radiosonde spectra at periods of 5.5–7 days (Fig. 1e) were presumed to derive from the inherent spatial and temporal smoothing of the model-based interpolation. However, one could not be certain that spatial variability did not introduce additional differences, which were magnified by the rather coarse $4^\circ \times 5^\circ$ representation of the ECMWF data. Figure 1 shows a comparison of (three point) smoothed v7 spectra for July and August 1987 and 1988 at grid points nearest Niamey from ECMWF analyses at each of the two resolutions as well as the v7 spectra for the station radiosonde observations. *It shows that the spectral signature is affected very little by the interpolation of the analyses to the coarser grid,* except that amplitudes are higher for the finer resolution. The periods of all of the major peaks are the same for both resolutions and, in fact, the correlation coefficients between the spectra in Figs. 1c and 1d and between the spectra in Figs. 1h and 1i are both 0.98, which has a near zero probability of being by chance. The correlation coefficients between each of the ECMWF spectra and the Niamey results (Figs. 1e,j) are somewhat lower: 0.82–0.85 for 1987 and 0.68–0.71 for 1988. Thus, differences between either of the ECMWF spectra and the Niamey spectra are larger than differences owing to resolution, sustaining the original assumption that the objective gridding procedure, regardless of the resolution, alters the properties of time series of the raw station data (Figs. 1e,j).

3. Horizontal fields

We also compared several ECMWF meteorological fields, used in the DLS study of AWDs, at the two resolutions over West Africa. The most striking impression was that maxima and minima of vertical motion and divergence took on a wider range of values at the higher resolution, although their spatial patterns were usually represented fairly well at $4^\circ \times 5^\circ$. Smaller differences were noted for distributions of specific humidity and horizontal circulation. The discussion below focuses on the atmospheric conditions for three selected synoptic times.

DLS described the synoptic conditions at 1200 UTC on 7 August 1988, immediately preceding the accumulation of some 29 mm of precipitation at Niamey (13°N, 2°E) during an 11-h period. According to our interpretation of ECMWF gridded analyses, this event was not AWD related. It was rather distinguished by a broad area of uplift in the midtroposphere ($\omega \equiv \Delta p/\Delta t < 0$, Figs. 2a,b), coupled with widespread upper-tropospheric divergence (DIV $\equiv \Delta u/\Delta x + \Delta v/\Delta y > 0$, Figs. 2c,d). Comparison of the analyses of these fields at both resolutions leads to the same conclusion as above regarding influences over Niamey. Elsewhere, the centers of vertical motion and divergence are somewhat stronger in the higher resolution representation, and $\omega < 0$ does not always coincide with DIV > 0.

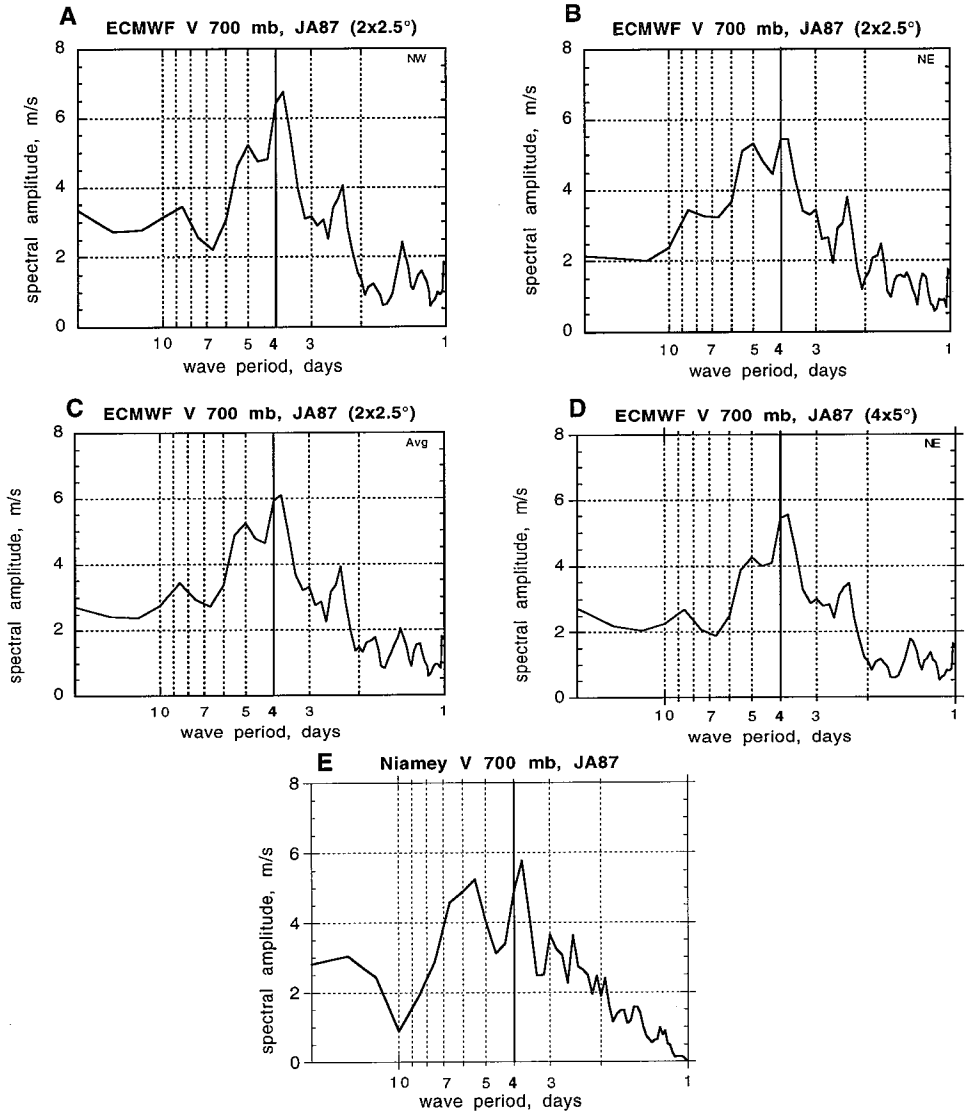

FIG. 1. Spectral amplitudes as a function of period for July and August time series of the 700-mb meridional wind. (a) Northwest of Niamey from ECMWF 2° × 2.5° resolution analyses, 1987; (b) northeast of Niamey from ECMWF 2° × 2.5° resolution analyses, 1987; (c) the average of (a) and (b); (d) northeast of Niamey from ECMWF 4° × 5° analyses, 1987; (e) Niamey station data; (f)–(j) like (a)–(d) but for 1988.

Some 12 h of rainfall at Niamey, straddling 0000 UTC 11 August 1988, preceded passage of an AWD trough later that day. The higher resolution analysis of 700-mb circulation (Figs. 3a, 4a) confirms that the trough line was east of the station at 0000 UTC. Moreover, the apparent incongruity of midtropospheric subsidence (Fig. 3), coinciding with strong low-level convergence just northeast of Niamey (Fig. 4), remains when the fields are depicted at 2° × 2.5° resolution. Figure 4b shows a schematic of vertical motion and divergence based on the 2° × 2.5° analyses at the standard pressure levels over the strong 850-mb convergence west of the AWD trough (18°N, 2.5°E) that was approaching Niamey.

Divergence associated with shear instabilities below the African easterly jet initiate rising motions within the lower troposphere. In Duvel's (1990) AWD composites, also based on ECMWF analyses, uplift ahead of troughs near 20°N is often confined to the lower layers. However, his composites for AWDs in the moist regime near 10°N indicate that large-scale vertical motion there often penetrates the midtroposphere, undoubtedly buoyed by the release of latent heat in moist convection. We now examine the vertical distribution of vertical motion associated with the analyses of 0000 UTC 11 August 1988.

Figures 5a–f show spatial distributions of the vertical motion ω at three levels based on analyses at both resolutions (for 0000 UTC 11 August 1988), each including a sketch of the AWD circulation (700 mb). In both re-

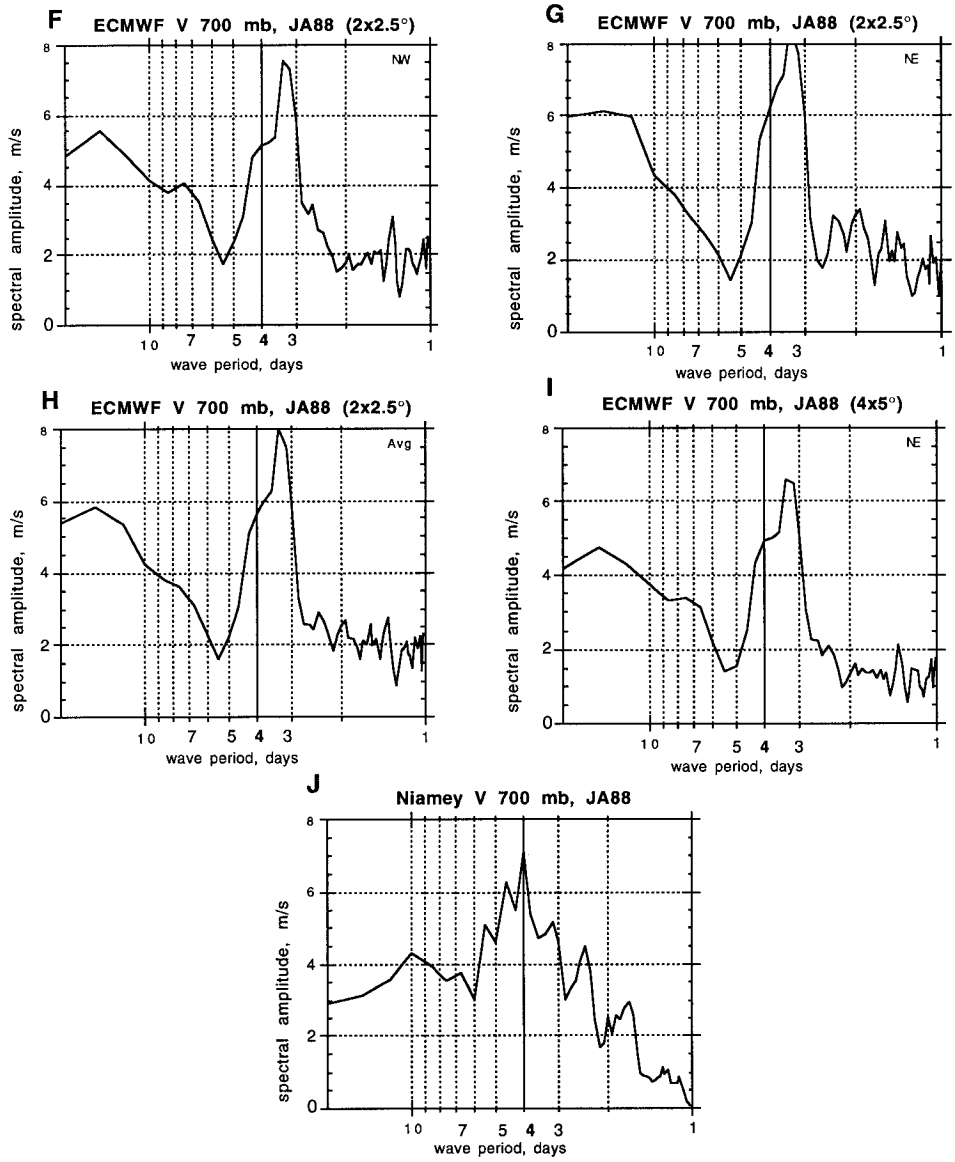

FIG. 1. (*Continued*)

presentations, ω maxima and minima were less extreme at 500 mb than at the lower two levels. In the lower troposphere, the coarser-resolution representations (Figs. 5b,c) indicate a single broad area of uplift from Niamey extending northwest almost to the coast. A very strong center of uplift at 20°N, 10°W was associated with what appears at this resolution to be a very gentle wave feature within the 700-mb circulation, overlying a closed cyclonic rotation of the 850-mb winds (Fig. 6b).

The analyses at 2° × 2.5° resolution (Figs. 5d–f) indicate that the two distinct centers of uplift over West Africa were separated by strong subsidence in the lower troposphere, implying that each of two African waves was creating bands of alternating ω of opposite sign. In particular, at both 850 and 700 mb, uplift was analyzed within the trough of the more northerly wave and downstream (west) of the more southerly wave trough. Strong midtropospheric uplift is shifted to the southwest of Niamey. Subsidence was situated east of the northerly trough but closer to the apex of the more southerly trough. In any case, rainfall at Niamey was consistent with the analysis of upward vertical motion within the lower troposphere (not examined in DLS), and not with the ω field at 500 mb, whose values varied from near zero over the station to positive values upstream, implying approaching subsidence. The schematic in Fig. 4b indicates that the confinement of strong uplift near Niamey to the lower troposphere may have been related to significant midtropospheric divergence.

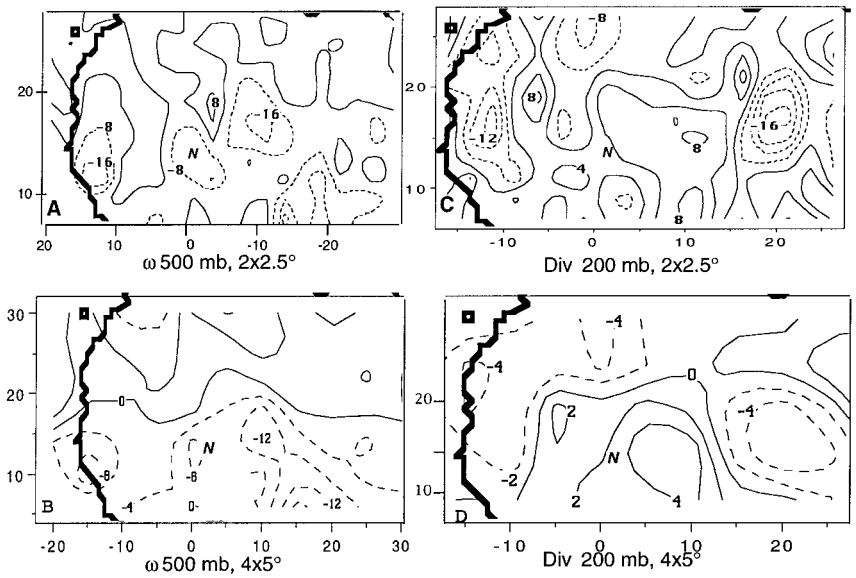

FIG. 2. Spatial distributions of 500-mb vertical motion ω (10^{-2} mb s^{-1}) and 200-mb divergence DIV2 (10^{-6} s^{-1}) at 1200 UTC 7 August 1988. (a) ω, ECMWF 2° × 2.5°; (b) ω, ECMWF 4° × 5°; (c) DIV2, ECMWF 2° × 2.5°; and (d) DIV2, ECMWF 4° × 5°. Broken lines indicate negative values and therefore uplift or convergence. The location of Niamey is indicated (N).

Spatial distributions of 850-mb circulation and specific humidity at this synoptic time are remarkably similar for both resolution analyses (Fig. 6).

Figures 7–10 show the spatial distribution of these same fields at 1200 UTC 15 August 1988, the midpoint of a heavy rain event at Niamey also associated with an AWD passage. Regarding the more southerly AWD, uplift associated with the trough and 850-mb convergence, as before, does not penetrate vertically to 500 mb according to analyses at both resolutions (Fig. 7). However, Figs. 9d–f suggest that the ω minimum near Niamey was tilted southwestward with altitude, perhaps explaining the seeming violation of mass continuity in the schematic representing conditions over 15°N, 5°E (Fig. 8b). The AWD trough was about 6° longitude east of Niamey at 1200 UTC (Fig. 8a), and vigorous uplift ahead of the trough in the lower layers was prompted by strong convergence at 1000 and 850 mb. This broad area of rising motion, apparently associated with the approaching AWD, was consistent with the observation of some 26 mm of precipitation at Niamey on 15 August 1988.

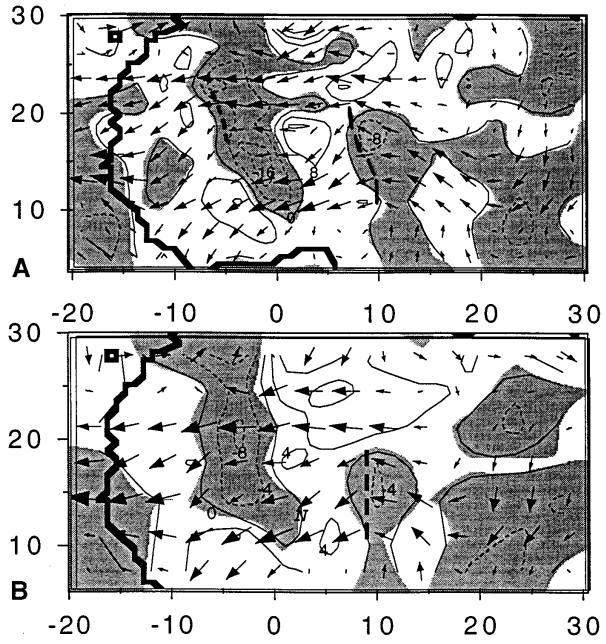

FIG. 3. Spatial distribution of 700-mb circulation (arrows) and 500-mb vertical motion (contours, 10^{-2} mb s^{-1}) at 0000 UTC 11 August 1988: (a) ECMWF 2° × 2.5° and (b) ECMWF 4° × 5°. Broken contours and shading indicate negative values and therefore uplift. Heavy broken lines mark AWD troughs and the location of Niamey is indicated (*N*).

Uplift associated with the more northerly AWD on 15 August 1988 (1200 UTC) extended at least to 500 mb (Fig. 9). Only the higher-resolution analysis shows that lower-tropospheric (850 and 700 mb) uplift occurred within the wave trough, relegating the subsidence to an area well east of the wave axis (Figs. 9e,f).

Duvel (1990) described the relative positions of lower-tropospheric convergence and wave troughs for two latitude swaths over West Africa, based on composites taken from ECMWF analyses representing the drought summers of 1983, 1984, and 1985. Duvel (1990) and Reed et al. (1977) have associated this convergence with convection and rainfall, but Duvel (1990) also showed that the growth of convective clouds is inhibited over the north-

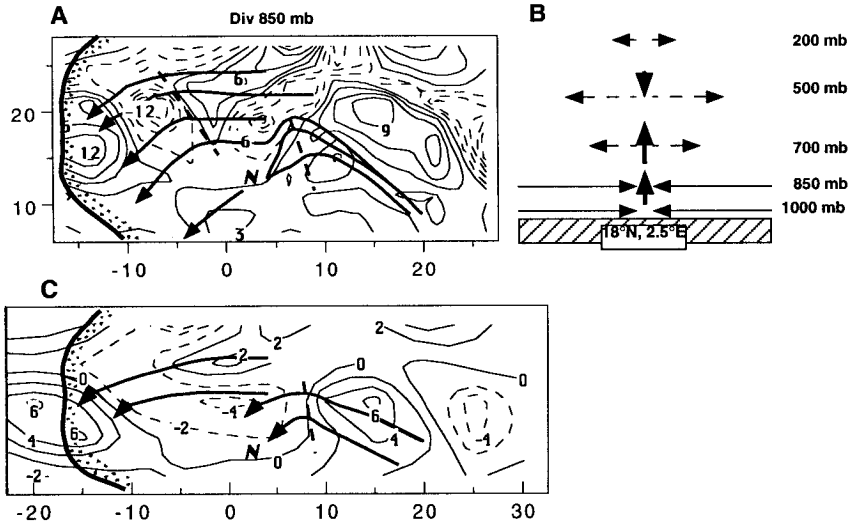

FIG. 4. (a) Spatial distribution of divergence at 850 mb (10^{-6} s^{-1}) at 0000 UTC 11 August 1988 for the ECMWF analysis at 2° × 2.5° horizontal resolution; (b) schematic showing relative strengths of vertical motion and divergence at standard levels over 18°N, 2.5°E, based on 2° × 2.5° analyses; (c) as in (a) but for 4° × 5°. Streamflow lines are based on the analyses of 700-mb winds shown in Fig. 3. Broken lines indicate negative values and therefore convergence. Heavy broken lines mark AWD troughs and the location of Niamey is indicated (*N*).

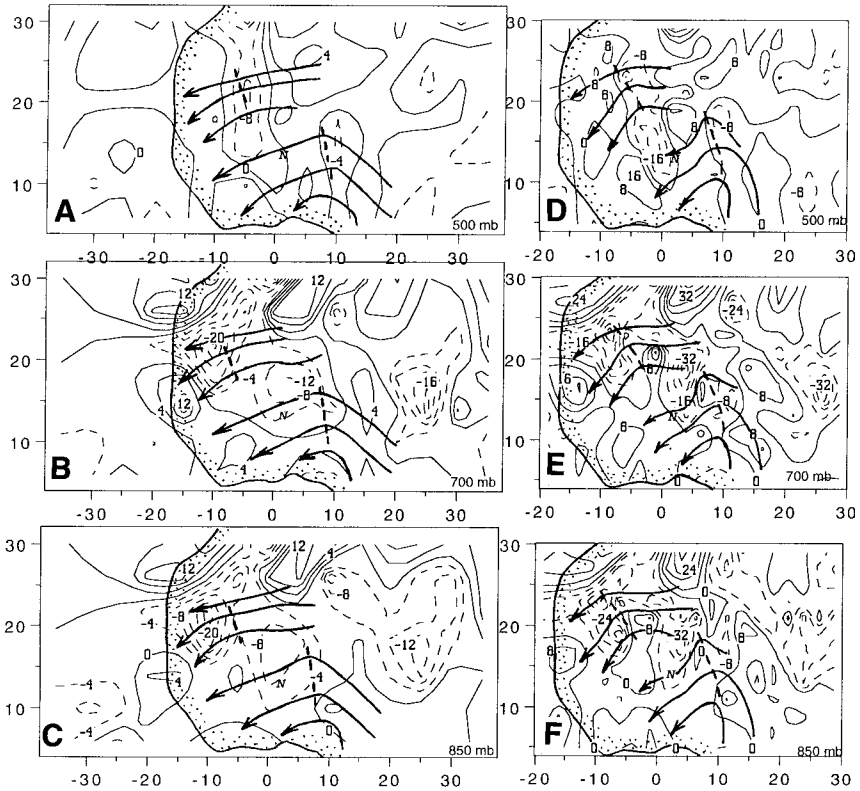

FIG. 5. Spatial distribution of vertical motion (10^{-2} mb s^{-1}) at three pressure levels at 0000 UTC 11 August 1988 for analyses at 4° × 5° horizontal resolution (a)–(c), and at 2° × 2.5° resolution (d)–(f). Streamflow lines are based on the analysis of 700-mb winds shown in Fig. 3. The location of Niamey is indicated (*N*).

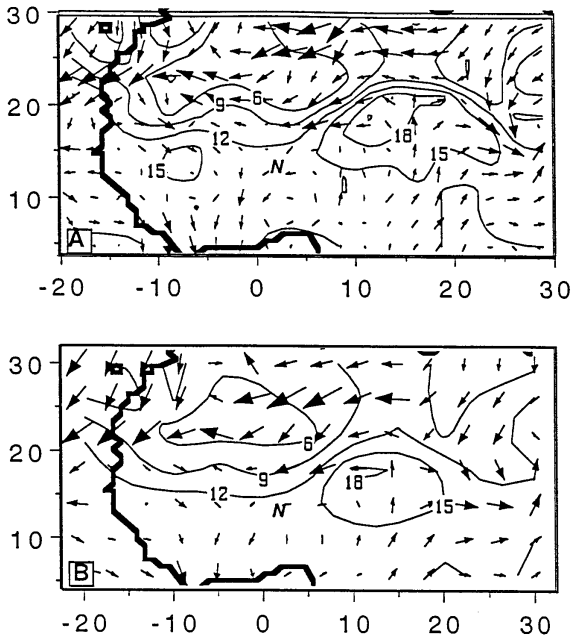

FIG. 6. Spatial distribution of 850-mb circulation (arrows) and specific humidity (g kg^{-1}) at 0000 UTC 11 August 1988: (a) ECMWF 2° × 2.5° and (b) ECMWF 4° × 5°. The location of Niamey is indicated (*N*).

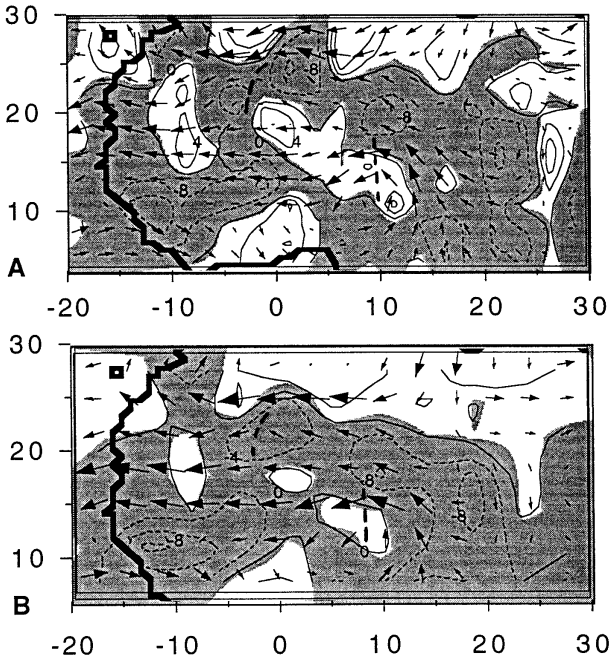

FIG. 7. Spatial distribution of 700-mb circulation (arrows) and 50-mb vertical motion (contours, 10^{-2} mb s^{-1}) at 1200 UTC 15 August 1988: (a) ECMWF 2° × 2.5° and (b) ECMWF 4° × 5°. Broken lines and shading indicate negative values and therefore uplift. Heavy broken lines mark AWD troughs and the location of Niamey is indicated (*N*).

ern Sahel where northerly circulation draws in very dry desert air, despite the convergence. DLS showed that such circumstances can also occur at Niamey.

Figures 4a and 8a offer the opportunity to examine the spatial distribution of 850-mb convergence associated with several AWDs during the relatively rainy month of August 1988 at the detail provided by the 2° × 2.5° resolution. In Fig. 4a, the trough of the more western AWD borders the eastern edge of one convergence center at 20°N, 7°W, while the second trough

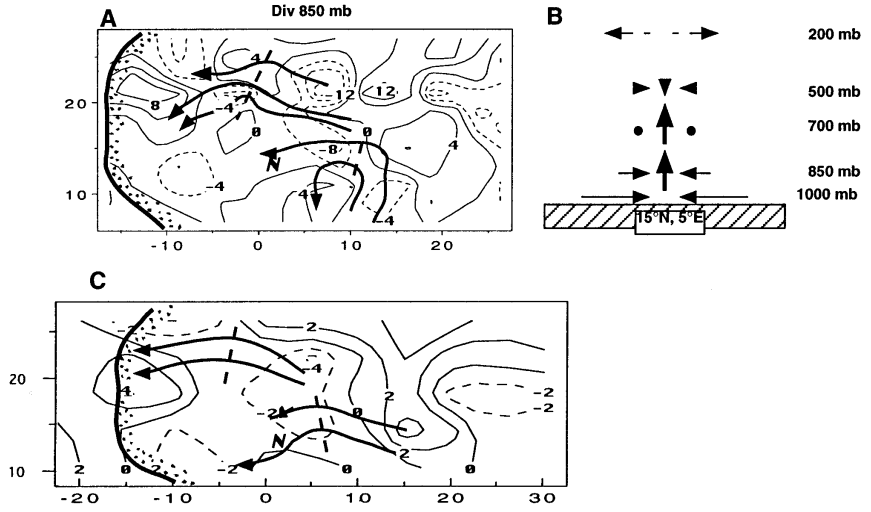

FIG. 8. (a) Spatial distribution of divergence at 850 mb (10^{-6} s^{-1}) at 12000 UTC 15 August 1988 for the ECMWF analysis at 2° × 2.5° horizontal resolution; (b) schematic showing relative strengths of vertical motion and divergence at standard levels over 15°N, 5°E, based on 2° × 2.5° analyses; (c) as in (a) but for 4° × 5°. Streamflow lines are based on the analyses of 700-mb winds shown in Fig. 7. Broken lines indicate negative values and therefore convergence. Heavy broken lines mark AWD troughs and the location of Niamey is indicated (*N*).

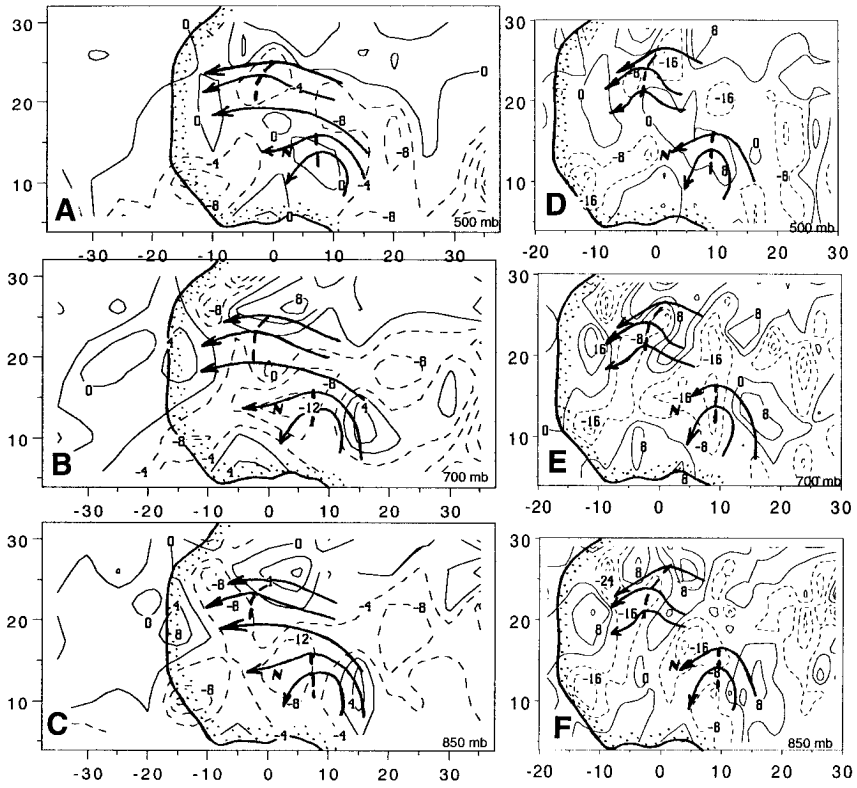

FIG. 9. Spatial distribution of vertical motion (10^{-2} mb s^{-1}) at three pressure levels at 1200 UTC 15 August 1988 for analyses at 4° × 5° horizontal resolution (a)–(c), and at 2° × 2.5° resolution (d)–(f). Streamflow lines are based on the analysis of 700-mb winds shown in Fig. 7. The location of Niamey is indicated (*N*).

borders the eastern edge of convergence centered at 18°N, 2.5°E. This juxtaposition conforms to Duvel's (1990) composites, which show convergence west of the AWD trough, but more detail is provided here by examination of the current case studies. For example, Fig. 4a shows that the convergence zones envelop the troughs, while the extremes are imbedded within the northeasterly circulation less than one-quarter wavelength to the west. Divergence brackets these areas on the upstream and downstream sides. The rather shallow wave at 20°N, 2.5°W in Fig. 8a is accompanied by a limited area of convergence just downstream of the trough and a more extensive area on the upstream side, separate features that are not well resolved at the coarser resolution (Fig. 8b). The more southerly AWD also features convergence areas running across the trough from the southeasterly to the northeasterly circulation. We do not know whether the convergence zones east of the troughs were associated with the dynamics of the AWD, but this morphology nevertheless does depart from the classical model depicted by compositing (Reed et al. 1977).

Figure 9 shows that at 1200 UTC 15 August 1988, vigorous upward vertical motion was analyzed at 850 and 700 mb over Niamey (reporting precipitation) and eastward to the adjacent AWD trough. As previously mentioned, this uplift did not reach 500 mb (Fig. 8b), but it appears to have been displaced southwestward with altitude (Fig. 9).

Reed et al. (1988b, Fig. 6c) show a north–south/vertical cross section of the variance of ω in a time series band passed for 3- to 4-day periods, based on ECMWF gridded data for August and September 1985. The maximum ω variance, interpreted as a manifestation of traversing AWD, was between 15° and 20°N at 850 mb, but tilted southward with altitude, reaching 9°N at 500 mb. Their results suggest that the waves' influence on vertical velocity diminishes rapidly with altitude directly above the strongest uplift between 850 and 700 mb. Rather, the region of modulated ω is tilted, reaching the midtroposphere at a horizontal displacement from the lower-tropospheric activity. We believe that the distributions of ω in Figs. 5 and 9, taken from August 1988, demonstrate this characteristic for two case studies.

To more systematically examine the vertical structure of vertical motion during rainfall events, we computed correlations between twice-daily precipitation accumulations at Niamey during July–September 1988, 244 observations in all, versus the corresponding ECMWF analyzed (at 2° × 2.5°) vertical motion at nearby grid points. Figure 11 shows the spatial distributions of the

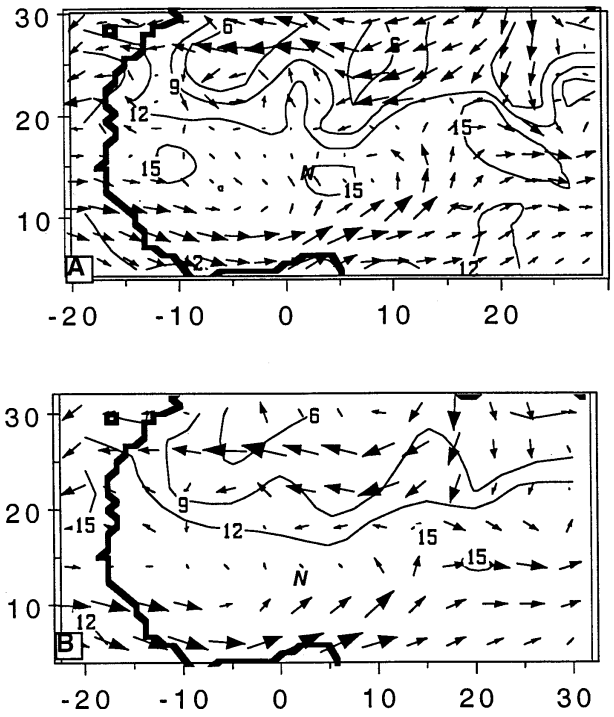

FIG. 10. Spatial distribution of 850-mb circulation (arrows) and specific humidity (g kg^{-1}) at 1200 UTC 15 August 1988: (a) ECMWF 2° × 2.5°, (b) ECMWF 4° × 5°. The location of Niamey is indicated (*N*).

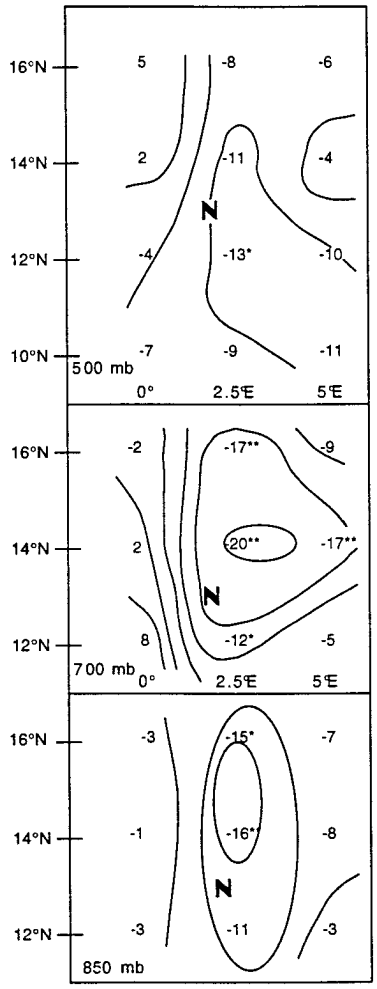

FIG. 11. Spatial distribution of correlation coefficients between twice-daily precipitation accumulations at Niamey July–September 1988 and corresponding values of ECMWF analyzed vertical motion at nearby grid points. Significance at the 99% confidence level is marked by double asterisks, at the 95% confidence level by single asterisks. The location of Niamey is indicated (*N*).

correlation coefficients in the vicinity of Niamey at 850, 700, and 500 mb, where negative values indicate the association of uplift with precipitation. Although all of the correlations are rather weak, several are significant at the 99% confidence level and several others at the 95% confidence level. Figure 11 shows that the correlations decrease away from the station, most rapidly to the west. The relationship is strongest at 700 mb and weakest at 500 mb, where high correlations are favored south of the station, recalling the vertical tilt of ω variance for August and September 1985 documented by Reed et al. (1988b). The correlation between the same precipitation time series and 700-mb vertical motion from the grid point northeast of Niamey in the 4° × 5° resolution analyses was −0.24, which is also significant at the 99% confidence level. However, because of the larger distances between grid points in the coarser resolution, no meaningful spatial pattern of correlation coefficients is evident.

By way of contrast, upward motion up to and including 500 mb was apparent near the trough of the more northerly AWD (Fig. 9). These particular examples do not fit the Duvel (1990) composite analyses, which found that uplift associated with AWD as far north as 20°N was more likely to to be shallow than uplift associated with AWD closer to 10°N. This discrepancy is probably due to Duvel's use of composite analysis, which averages the features of a number of AWDs. Thus, uplift at a particular level in one wave, averaged with subsidence in another wave, can produce near zero vertical motion in the composite. A strong motivation for diagnosing individual cases, as in this study, is that the integrity of unique wave structures is preserved in the analysis.

The GISS GCM has been used to study AWDs, primarily at 4° × 5° grid resolution (Druyan and Hall 1994, 1996), although a single simulation has now been analyzed from a version with comparable physics run at 2° latitude by 2.5° longitude horizontal resolution. It is instructive to compare differences in simulated AWDs at the two horizontal resolutions with some of the analyzed differences discussed above. Figure 12a shows spatial distributions of divergence (at approximately 890 mb) and horizontal circulation, which includes an AWD (at approximately 780 mb) from an arbitrarily chosen

model integration for August at the coarser resolution. The same fields from the 2° × 2.5° run are shown in Fig. 12b. Both simulated AWD feature lower-tropospheric convergence southwest of the wave apex and divergence east of the troughs, as in the ECMWF analyses (Figs. 4 and 8). However, the divergence extremes are considerably stronger in the higher-resolution version, which also reveals a sharp transition from convergence to divergence at the trough line. These features reflect the effects of integration on the higher-resolution grid, including sharper horizontal gradients of model variables and of surface topography, and are not mere by-products of interpolation, as in the case of the ECMWF analyses. Although this is but a single example, these parallels between resolution effects for analyses and simulations lend confidence to their meteorological significance, and they demonstrate some of the advantages gained by the finer grid.

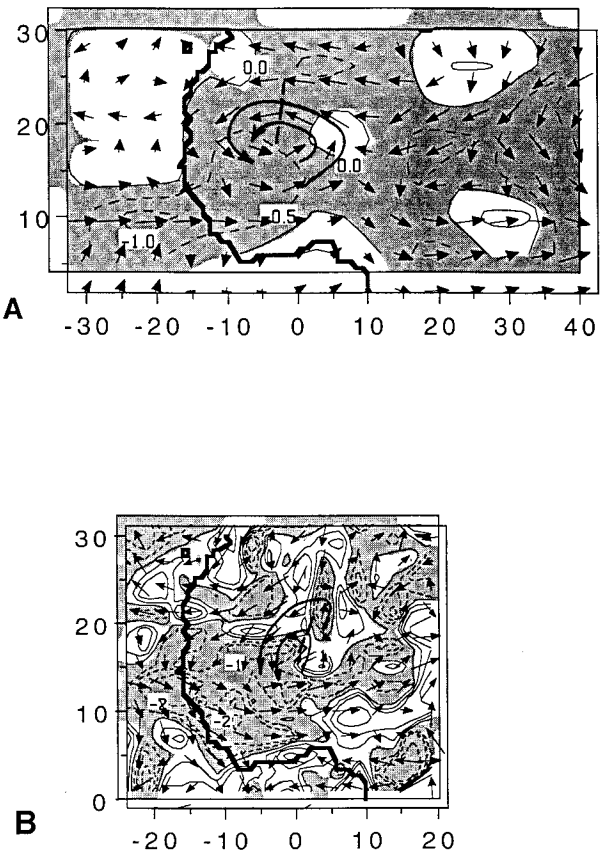

FIG. 12. Spatial distribution of simulated 780-mb circulation (arrows) and divergence at 890 mb (10^{-5} s^{-1}) by GISS GCM. Computational grid resolutions: (a) 4° latitude by 5° longitude and (b) 2° latitude by 2.5° longitude.

4. Conclusions

Several synoptic situations associated with summer rainfall at Niamey (Niger) have been examined. We found that ECMWF analyses gridded at 4° × 5° horizontal resolution depict the gross features of circulation associated with AWDs over West Africa, which can be confirmed by comparing them with the corresponding datasets gridded at 2° × 2.5° resolution. Even at the higher resolution, analyzed vertical motion patterns at 500 mb are not well correlated with areas of low-level convergence, AWD troughs, or ω at lower levels. Previous studies showed that 500 mb is not the level of maximum vertical motion associated with AWD. In two AWD-related Niamey rain events discussed here, uplift over the station was most pronounced within the lower troposphere and was displaced to the southwest at 500 mb. Significant correlations between Niamey rainfall and analyzed vertical motion, especially at 700 mb, reflect the influence of the occasional synoptic event, such as depicted in the above case studies, as a trigger for precipitation at the station. The weakness of the correlations, however, indicates that many rainfall events are not necessarily timed with the most extreme values of analyzed uplift, either because of the variability of available moisture or because mesoscale convection can be dissociated from broad-scale patterns.

Two AWD analyzed here at higher latitudes (near 20°N) showed less vertical tilt to the zone of uplift than their more southerly counterparts, contrary to a previous finding. Analyses based on the higher-resolution data and the higher-resolution GCM simulation resolve other somewhat finer features of midtropospheric waves, showing sharp transitions between lower-tropospheric convergence (divergence) and uplift (subsidence) across wave troughs. There were also examples showing 850-mb convergence and uplift situated within troughs.

The study shows that the spatially coherent and time-continuous data provided by model-generated analyses and simulations are useful for investigating the behavior of individual AWD. While generalizations are best supported by the summary of many examples, the analysis of individual case studies preserves features of distinctive systems that can be hidden by composites on which previous models of AWDs have been based.

Acknowledgments. This research is supported by NSF ATM-9407018 (LD), NASA Grant NAGW 4163 (JC), and the NASA Climate and Earth Observing System Programs. ECMWF data were provided courtesy of Dr. C.-K. Park and technical assistance in data handling by S. Kaltenbaugh, both of the NASA/Goddard Space Flight Center. M. Saloum of the Direction Météorologie Nationale du Niger supplied hourly precipitation observations for Niamey. Discussions with Dr. R. Miller were very helpful.

REFERENCES

Burpee, R. W., 1972: The origin and structure of easterly waves in the lower troposphere of North Africa. *J. Atmos. Sci.,* **29,** 77–90.

Druyan, L., and T. Hall, 1994: Studies of African wave disturbances with the GISS GCM. *J. Climate,* **7,** 261–276.

——, and ——, 1996: The sensitivity of African wave disturbances to remote forcing. *J. Appl. Meteor.*, **35,** 1100–1110.

——, P. Lonergan, and M. Saloum, 1996: African wave disturbances and precipitation at Niamey during July–August 1987 and 1988. *Climate Res.*, **7,** 71–83.

Duvel, J., 1988: Analysis of diurnal, interdiurnal and interannual variations during Northern Hemisphere summers using METEOSAT infrared channels. *J. Climate*, **1,** 471–484.

——, 1990: Convection over tropical Africa and the Atlantic Ocean during northern summer. Part II: Modulation by easterly waves. *Mon. Wea. Rev.*, **118,** 1855–1868.

Fortune, M., 1980: Properties of African squall lines inferred from time-lapse satellite imagery. *Mon. Wea. Rev.*, **108,** 153–168.

Lamb, P., and R. Peppler, 1991: West Africa. *Teleconnections: Linkages Between ENSO, Worldwide Climate Anomalies, and Societal Impacts*, M. H. Glantz, R. W. Katz, and N. Nicholls, Eds., Cambridge University Press, 121–189.

Landsea, C., and W. Gray, 1992: The strong association between Western Sahelian monsoon rainfall and intense Atlantic hurricanes. *J. Climate*, **5,** 435–453.

Reed, R., D. Norquist, and E. Recker, 1977: The structure and properties of African wave disturbances as observed during Phase III of GATE. *Mon. Wea. Rev.*, **105,** 317–333.

——, A. Hollingsworth, W. Heckley, and F. Delsol, 1988a: An evaluation of the performance of the ECMWF operational system in analyzing and forecasting easterly wave disturbances over Africa and the tropical Atlantic. *Mon. Wea. Rev.*, **116,** 824–865.

——, E. Klinker, and A. Hollingsworth, 1988b: The structure and characteristics of African easterly wave disturbances as determined from the ECMWF operational analysis/forecast system. *Meteor. Atmos. Phys.*, **38,** 22–33.

Trenberth, K. E., 1992: Global analyses from ECMWF. National Center for Atmospheric Research TN-373+STR, 191 pp. [Available from NCAR, P.O. Box 3000, Boulder, CO 80307-3000.]